

“Role Of Contrast Enhanced Computed Tomography In Cervical Lymphadenopathy In Head and Neck Malignancy”

Dr. Disha Mittal*, Dr. Sanjay Dhawan**,

*Department of Radiodiagnosis, Assistant Professor (PGIMS Rohtak) India.

**Department of Radiodiagnosis, Consultant Radiologist Paras Hospital, Gurugram, Haryana, India.

Abstract:

Introduction: Nodal metastases have a great impact on treatment and prognosis in head and neck cancer. This study aimed to assess the findings of contrast enhanced computed tomography (CECT) findings in enlarged malignant cervical lymph nodes with histopathological / cytopathological correlation and to identify the site of primary tumor in metastatic lymph nodes wherever possible.

Materials and Methods: We evaluated 150 cases. CECT findings including distribution, size, shape, outline, hilum, internal architecture, calcification, intranodal necrosis, matting, enhancement pattern and final diagnosis. All of CECT findings were correlated with cytopathological/ histopathological findings.

Results: CECT Findings: Out of 150 cases, 93 (62%) were malignant-metastases in 66 (44%) and lymphoma in 27 (18%). In our study, 63.6% (42/66) of metastatic nodes were unilateral. Short axis > 10 mm was seen in 72.7% (48/66) of metastatic lymph nodes. In our study 90.9% (60/66) of metastatic lymph nodes were round. Blurring of margins, suspicious of extranodal extension was seen in 31.8% (21/66) metastatic lymph nodes, Hilum was absent in 86.4% metastatic lymph nodes, In metastatic lymph nodes most common pattern was CLD 45.5% followed by LCLD 31.8% and HSTD 18.2% (CLD-central low density, HSTD-homogeneous soft tissue density, LCLD-large confluent low density). Necrosis was present in 81.8% cases of metastatic lymph nodes. Matting was found in 50% (33/66) cases of metastatic lymph nodes. Calcification was seen in 9.1 % cervical lymph nodes. In our study 27.3% (18/66) of metastatic lymph nodes were showing peripheral enhancement.

Conclusion: CECT is an important imaging tool in early detection of metastatic nodes for minimizing morbidity and avoiding elective neck dissection and staging of metastatic cervical lymphadenopathy. CECT is useful in predicting the primary site of malignancy and in follow up in patients of metastatic lymphadenopathy.

Key words: Cervical lymphadenopathy, contrast enhanced computed tomography, malignant nodes.

Date of Submission: 29-05-2019

Date of acceptance: 15-06-2019

I. Introduction

Nodal metastases have a great impact on treatment and prognosis in head and neck cancer.¹ Contrast enhanced computed tomography (CECT) is the preferred investigation of lymph nodal disease of neck.¹

Metastatic cervical lymph nodes are site specific. In patients with a known primary tumor, the distribution of metastatic nodes helps to identify metastases and assists tumor staging. However, if the primary tumor is not identified, the distribution of proven metastatic nodes may give a clue to identify the primary.²⁻⁴ The early detection of lymph node metastases is important because it could affect the survival rate of cancer patients.⁵

Diagnosis based on imaging evaluation of nodal size is more accurate than diagnosis based on palpation alone because CT can show lymph nodes that are not accessible to palpation (retropharyngeal, tracheoesophageal and those deep to the sternocleidomastoid muscles).¹

II. Aims And Objectives

1-To evaluate the contrast enhanced computed tomography (CECT) findings in enlarged malignant cervical lymph nodes with histopathological / cytopathological correlation.

2-To evaluate the efficacy of contrast enhanced computed tomography in detecting malignant cervical lymphadenopathy.

3- To identify the site of primary tumor in metastatic lymph nodes wherever possible.

III. Materials And Methods

All the cases suspected of having cervical lymphadenopathy or patient with suspected or known primary in the neck referred for CECT evaluation of the neck were included in the study. Cases for which cytopathological/histopathological correlation could not be obtained, were excluded from the study.

CECT Protocol: CT was performed on Siemens Somatom Sensation 64 Cardiac CT. Non ionic contrast 60-90 ml was used intravenous depending upon weight of the patient. Patient selection was based on previous inclusion-exclusion criteria. A consent was taken from all patients before conducting the CECT. CT neck was performed using spiral scanning at 3mm thickness and 3mm increments with 0.6 x 64 mm collimation and pitch of 1. The scan was acquired from the base of skull to arch of aorta with the patient in supine position. Contrast was administered and images were acquired and reconstructed using a Standard algorithm and Bone algorithm. Scan time ranged between 12sec-15sec with a peak voltage of 120 KVp and effective tube current of 200-240 mAs. Images were saved and evaluated at a window width of 250 Hounsfield units (HU) and a window level of 50 HU.

CECT findings including distribution, Anatomical site {According to imaging based nodal classification (adopted from Som P.M. Curtin H.D. Mancuso A.A.)⁶} (Table-1), size, shape (oval/round), outline, hilum, internal architecture, calcification, intranodal necrosis, matting, enhancement pattern and final diagnosis.

Statistical Analysis: Data was analyzed using software SPSS version 15 statistical analysis software. The values were represented in number (percent) and Mean \pm SD. Chi square test, ANOVA, Fisher exact test and unpaired student's t-test were used. p-value less than 0.05 was considered as significant.

All of CECT findings were correlated with cytopathological / histopathological findings.

IV. Results

Total 150 cases of cervical lymphadenopathy were evaluated in the study. According to final cytopathological/histopathological diagnosis, out of 150 cases, 93 (62%) were malignant-metastases in 66 (44%) and lymphoma in 27 (18%) cases. Neck swelling was the commonest complaint in all cases of cervical lymphadenopathy. The commonest complaint was neck swelling in all cases of cervical lymphadenopathy.

CECT Findings In Malignant Cervical Lymphadenopathy (Table-2):

In present study level II was commonest to be involved. For location IV and VI, the proportion of lymphoma groups was significantly higher as compared to other groups ($p < 0.05$). In our study, 63.6% (42/66) of metastatic nodes were unilateral. Out of 27 cases 15 cases of lymphomatous nodes were bilateral. Short axis > 10 mm was seen in 72.7% (48/66) metastatic lymph nodes and 88.9% (24/27) of lymphomatous nodes. In our study 90.9% (60/66) of metastatic and 66.7% (18/27) of lymphomatous lymph nodes were round. Blurring of margins, suspicious of extranodal extension was seen in 31.8% (21/66) of metastatic lymph nodes, and 22.2% (6/27) lymphomatous nodes. Hilum was absent in 86.4% (57/66) of metastatic lymph nodes, and 100% (27/27) lymphomatous nodes. Majority of metastatic lymph nodes were with central low density (CLD) 45.5% (30/66) followed by large confluent low density (LCLD) 31.8% (21/66), homogeneous soft tissue density (HSTD) 18.2% (12/66) and multilobular central low density (MCLD) 4.5% (3/66). Among internal architecture findings, homogeneous soft tissue density (HSTD) was more common in lymphoma groups as compared to the malignant groups ($p = 0.021$). Other findings were not statistically significant.

Calcification was found in 9.1% (6/66) of metastatic lymph nodes and 22.2% (6/27) of lymphomatous nodes (3 were untreated non-Hodgkin's lymphoma and 3 were Hodgkin's lymphoma). Necrosis was present in 81.8% (54/66) of metastatic lymph nodes, 22.2% (6/27) of lymphomatous nodes. Incidence of necrosis was found to be significantly higher among metastatic groups as compared to other groups ($p = 0.021$). Matting was found in 50% (33/66) cases of metastatic lymph nodes, 22.2% (2/27) of lymphomatous nodes.

Homogeneous enhancement was seen in 31.8% (21/66) metastatic lymph nodes and peripheral enhancement was seen in 27.3% (18/66) of metastatic lymph nodes. In our study 44.4% (12/27) of lymphomatous lymph nodes were non enhancing while they have homogeneous and peripheral enhancement in 44.4% (12/27) and 11.1% (3/27) cases respectively. On enhancement, the incidence of non enhancing pattern (N) was significantly higher in lymphoma groups as compared to metastatic groups ($p = 0.007$).

Detection of primary site in metastatic lymph nodes on CECT:

In our study out of the 24 patients with unknown primary, who had metastatic cervical lymph nodes, CT suggested the primary site in 18 cases which was later confirmed on cytopathology/histopathology. In the remaining 6 cases, no primary site was suspected even on CT (Table 3).

V. Discussion

CECT has limited role in diagnosing metastatic nodes. Most significant features for differentiating between various pathologies on CECT were shape and necrosis.

Lymphadenopathy was more common in the level II suggesting that it is the most commonly involved nodal chain. Pattern and level of lymph nodes can help to suggest the site of primary cancer in unknown primary (Table 3). CECT is good modality to detect primary site in a case of unknown primary.⁷ It was able to predict the primary site in 75% cases.

According to RECIST 1.1, to be considered pathologically enlarged and measurable, a lymph node must be at least 15mm in short axis when assessed by CT scan. Lymph nodes that are at least 10mm but less than 15mm in short axis may be pathologic and can be considered non-measurable/nontarget lesions.⁸

Nodes less than 1 cm in size should be carefully evaluated for other abnormal features, particularly if they are in expected drainage sites of the primary tumor because they can still be malignant.¹ Small nodes can harbor small metastases that do not expand the node, and, conversely, benign nodes can commonly be enlarged due to hyperplasia or inflammation.¹

Metastatic nodes tend to be round with a short to long axes ratio (S/L ratio) greater than 0.5, while reactive or benign lymph nodes are elliptical in shape (S/L ratio 50.5).⁹ Round shape was more common in metastatic group as compared to lymphoma groups in present study (p=0.001).

Imaging findings of extracapsular spread are irregular margins, fat stranding, and loss of fat planes with adjacent structures.¹ Extra nodal neoplastic spread occurs even in small nodes and early extra nodal spread can be used as a diagnostic sign of a malignant node.¹ Diagnostic accuracy is similar on MRI and CT.¹⁰ In our study, 31.8% cases of metastatic lymph nodes showed extracapsular spread while Sarvanan et al (2002) found extracapsular spread in 15% of metastatic lymph nodes.¹¹

Metastatic, lymphomatous and tuberculous nodes usually does not have hilum but they may present with an echogenic hilum in their early stage of involvement.¹² Some authors have reported that hyperechoic hilum was visualized in up to 51.5% of metastatic nodes.¹³ Homogeneous soft tissue density was more common in lymphomatous nodes as compared to the malignant lymph nodes (p=0.021).

Calcification within lymph nodes is uncommon, however, metastatic cervical nodes from papillary carcinoma of the thyroid tend to show calcification.¹ It is documented in previous study that Hodgkin's lymphoma nodes treated with irradiation or chemotherapy may calcify.^{14,15} Calcification was also reported in untreated Hodgkin's lymphoma and non Hodgkin's lymphoma.^{16,17}

The most valuable CT criterion for the presence of metastatic lymphadenopathy is central necrosis.¹⁸ CECT is considered to be the good modality for identification of necrosis. Necrosis was seen in 80% of metastatic lymph nodes. A sensitivity of 74% and a specificity of 94% have been reported for areas of necrosis larger than 3 mm.¹¹ Incidence of necrosis was found to be significantly higher among metastatic group as compared to other groups in our study (p=0.021). Sarvanan et al (2002) showed matting in 23% cases of metastatic nodes.¹¹

Heterogeneous enhancement pattern was most specific for metastatic lymph nodes. Sakaguchi et al found homogeneous enhancement in 19% and peripheral enhancement in 35% of metastatic lymph nodes.¹⁹

On CECT, out of 150 cases 90 were detected to be malignant and 60 were detected to be benign. However, there were 9 false negative malignant and 6 false positive malignant. Overall the sensitivity of CECT was 90.3% and specificity was 89.5%. The positive predictive value for malignancy was 93.3% while negative predictive value was 85%. Overall diagnostic accuracy was 90%. Our results were comparable to previous study which reported sensitivity and specificity of CECT in the evaluation of metastatic cervical lymph nodes 90.2% and 93.9% respectively.²⁰

There were also few drawbacks in our study

- Exact distribution and morphology of the lymph nodes could not be studied due to small sample size.
- In our study few results were contradictory to previous published studies which also could be due to small sample size and non uniformity of selection of metastatic and lymphoma cases.

VI. Conclusion

To evaluate cervical lymphadenopathy in head and neck malignancy, an organized approach is needed. CECT is an important imaging tool in early detection of metastatic nodes for minimizing morbidity and avoiding elective neck dissection and staging of metastatic cervical lymphadenopathy.

CECT is useful in predicting the primary site of malignancy and in follow up in patients of metastatic lymphadenopathy. However, CECT lacks the ability to evaluate the internal architecture of nodes as compared to USG, still helpful to differentiate benign from malignant causes of lymphadenopathy.

References

- [1]. Jenny K. Hoang, Jyotsna Vanka, Benjamin J. Ludwig, Christine M. Glastonbury. Evaluation of Cervical Lymph Nodes in Head and Neck Cancer With CT and MRI: Tips, Traps, and a Systematic Approach. *AJR* 2013; 200:W17–W25.
- [2]. Van den Brekel MWM, Stel HV, Castelijns JA. Cervical lymph node metastasis: Assessment of radiologic criteria. *Radiology* 1990; 177: 379-84.
- [3]. Van den Brekel MWM, Castelijns JA, Snow G. Detection of lymph node metastases in the neck: radiologic criteria. *Radiology* 1994; 192: 617-8.
- [4]. Shah JP, Cendon RA, Farr HW, Strong EW. Carcinoma of the oral cavity: factors affecting treatment failure at the primary site and neck. *Am J Surg* 1976; 132: 504-7.

[5]. PT Figueiredo*,1, AF Leite1, AC Freitas2, LA Nascimento3, MG Cavalcanti4, NS Melo5 and EN Guerra5. Comparison between computed tomography and clinical evaluation in tumour/node stage and follow-up of oral cavity and oropharyngeal cancer. Dentomaxillofacial Radiology (2010) 39, 140–148.

[6]. Som PM, Curtin HD, Mancuso AA. Imaging based nodal classification for evaluation of neck metastatic adenopathy. Am J Roentgenol 2000; 174: 837-44.

[7]. Regelink G, Brouwer J, de Bree R, et al. Detection of unknown primary tumours and distant metastases in patients with cervical metastases: value of FDG-PET versus conventional modalities. Eur J Nucl Med Mol Imaging. 2002; 29: 1024-30.

[8]. Schwartz LH, Bogaerts J, Ford R, et al. Evaluation of lymph nodes with RECIST 1.1. Eur J Cancer 2009; 45:261-267.

[9]. Ahuja AT, Ying M, Ho SY, Antonio G, Lee YP, King AD, et al. Ultrasound of malignant cervical lymph node. Cancer Imaging 2008; 8: 48-56.

[10]. Ahuja A, Ying M. An overview of neck node sonography. Invest Radiol 2002; 37: 333-42.

[11]. Sarvanan K, Bapuraj JR. Computed tomography and ultrasonographic evaluation of metastatic cervical lymph nodes with surgicoclinicopathologic correlation. J Laryngol Otol 2002; 116(3): 194-9

[12]. Evans RM, Ahuja A, Metreweli C. The linear echogenic hilus in cervical lymphadenopathy - a sign of benignity or malignancy? Clin Radiol 1993; 47: 262-4.

[13]. Vassallo P, Wernecke K, Roos N, Peters PE. Differentiation of benign from malignant superficial lymphadenopathy: the role of high resolution. US Radiol 1992; 183: 215-20.

[14]. Strijk SP. Lymph node calcification in malignant lymphoma: Presentation of nine cases and a review of literature. Acta Radiol Diag (Stockh) 1985; 26: 427-31.

[15]. Williams MP, Cheryman GR. Lymph node calcification in Lennert’s lymphoma. Br J Radiol 1987; 60: 1131-2.

[16]. Wycoco D, Raval B. An unusual presentation of mediastinal Hodgkin’s lymphoma on computed tomography. J Comput Tomogram 1983; 7: 187-188.

[17]. Ahuja A, Ying M. Sonography of neck lymph nodes. Part II: Abnormal lymph nodes. Clin Radiol 2003; 58: 359-66.

[18]. Kaji AV, Mohuchy T, Swartz JD. Imaging of cervical lymphadenopathy. Semin Ultrasound CT MR 1997; 18:220-249.

[19]. Sakaguchi T, Yamashita Y, Katahira K, Nishimura R, Baba Y, Arakawa A, et al. Differential diagnosis of small round cervical lymph nodes: comparison of power doppler US with contrast-enhanced CT and pathologic results. Radiation Med 2001; 19(3): 119-25.

[20]. Jeong HS, Baek CH, Son YI, Ki Chung M, Kyung Lee D, Young Choi J, et al. Use of integrated 18F-FDG PET/CT to improve the accuracy of initial cervical nodal evaluation in patients with head and neck squamous cell carcinoma. Head Neck 2007; 29: 203-10.

Table 1: An Imaging based nodal classification (adapted from Som P.M., Curtin H.D, Mancuso A.A.)⁶ is now widely used for reporting of CT scan of neck (Figure 1).

Level	Definition of nodes
I	Above hyoid bone Below mylohyoid muscle Anterior to back of submandibular gland
IA	Between medial margins of anterior bellies of digastric muscles Previously classified as submental nodes
IB	Posterolateral to level IA nodes Previously classified as submandibular nodes
II	From Skull base to level of lower body of hyoid bone Posterior to back of submandibular gland Anterior to back of sternocleidomastoid muscle
IIA	Anterior, lateral, medial, or posterior to internal jugular vein Inseparable from internal jugular vein (if posterior to vein) Previously classified as upper internal jugular nodes
IIB	Posterior to internal jugular vein with fat plane separating nodes and vein Previously classified as upper spinal accessory nodes
III	From level of lower body of hyoid bone to level of lower cricoid cartilage arch Anterior to back of sternocleidomastoid muscle Previously known as mid jugular nodes
IV	From level of lower cricoid cartilage arch to level of clavicle Anterior to line connecting back of sternocleidomastoid muscle and posterolateral margin of anterior scalene muscle Lateral to carotid arteries Previously known as low jugular nodes
V	Posterior to back of sternocleidomastoid muscle from skull base to level of lower cricoid arch. From level of lower cricoid arch to level of clavicle as seen on each axial scan. Posterior to line connecting back of sternocleidomastoid muscle and posterolateral margin of anterior scalene muscle. Anterior to anterior edge of trapezius muscle
VA	From skull base to level of bottom of cricoid cartilage arch Posterior to back of sternocleidomastoid muscle Previously known as upper level V nodes
VB	From level of lower cricoid arch to level of clavicle as seen on each axial scan Posterior to line connecting back of sternocleidomastoid muscle and posterolateral margin of anterior scalene muscle Previously known as lower level V nodes
VI	Between carotid arteries from level of lower body of hyoid bone to level

	superior to top of manubrium Previously known as visceral nodes
VII	Between carotid arteries below level of top of manubrium Caudal to level of innominate vein Previously known as superior mediastinal nodes
Supraclavicular	At or caudal to level of clavicle as seen on each axial scan Above and medial to ribs
Retropharyngeal	Within 2 cm of skull base and medial to internal carotid arteries

n=no of patients, L/S=long axis/short axis.

Sensitivity=74.2%, Specificity = 84.2%, PPV = 88.5%, NPV = 66.7%; DA=78.0%

Table 2: Morphological features of cervical lymphadenopathy on CECT

Features	Meta-static (n=22)	Lymphoma (n=9)	Level of Significance
Distribution			
Bilateral	24 (36.4%)	45 (55.6%)	p=0.756
Unilateral	42 (63.6%)	36 (44.4%)	
Size(short axis) >10 mm	48 (72.7%)	24 (88.9%)	p=0.702
Size (Mean±SD)	0.73±0.46	0.89±0.33	p=0.201
L/S ratio (Mean±SD)	1.60±1.05	1.63±0.51	p=0.655
Shape			
Oval	6 (9.1%)	9 (33.3%)	p=0.001
Round	60 (90.9%)	18 (66.7%)	
Margins			
Blurred	21 (31.8%)	6 (22.2%)	p=0.299
Well defined	45(68.1%)	21(77.8%)	
Hilum			
Lost	57 (86.4%)	27 (100%)	p=0.682
Present	9 (13.6%)	0	
Internal architecture			
CLD	30 (45.5%)	6 (22.2%)	p=0.080
HSTD	12 (18.2%)	15 (55.6%)	p=0.0021
LCLD	21 (31.8%)	6 (22.2%)	p=0.948
MCLD	3 (4.5%)	0	p=0.729
Calcification	6 (9.1%)	6 (22.2%)	p=0.245
Necrosis	54 (81.8%)	12 (44.4%)	p=0.021
Matting	33 (50.0%)	6 (22.2%)	p=0.414
CT Enhancement			
Homogeneous	21 (31.8%)	12 (44.4%)	p=0.244
Heterogeneous	27 (4.5%)	0	p=0.729
Absent	0	12 (44.4%)	p=0.007
Peripheral	18 (27.3%)	3 (11.1%)	p=0.011

CLD-central low density, HSTD-homogeneous soft tissue density, LCLD-large confluent low density, MCLD-multilocular central low density, L/S=long axis/short axis, SD-standard deviation.

Table 3: Primary site suggested by CECT in case of unknown primary

Level of Lymph nodes	Site Suggested	Confirmed on biopsy
L IB,II	Oral Cavity	Oral Cavity
RIIA,	Oropharynx	Tonsil
RIIA(III)	Oropharynx	Base of tongue
LII,III,IV	Oropharynx/hypopharynx	Oropharynx
R IIA(VA)	Supraglottic	Supraglottic
LIA,IB,II	Oral Cavity	Buccal mucosa

Figure 1: Diagnostic efficacy of CECT

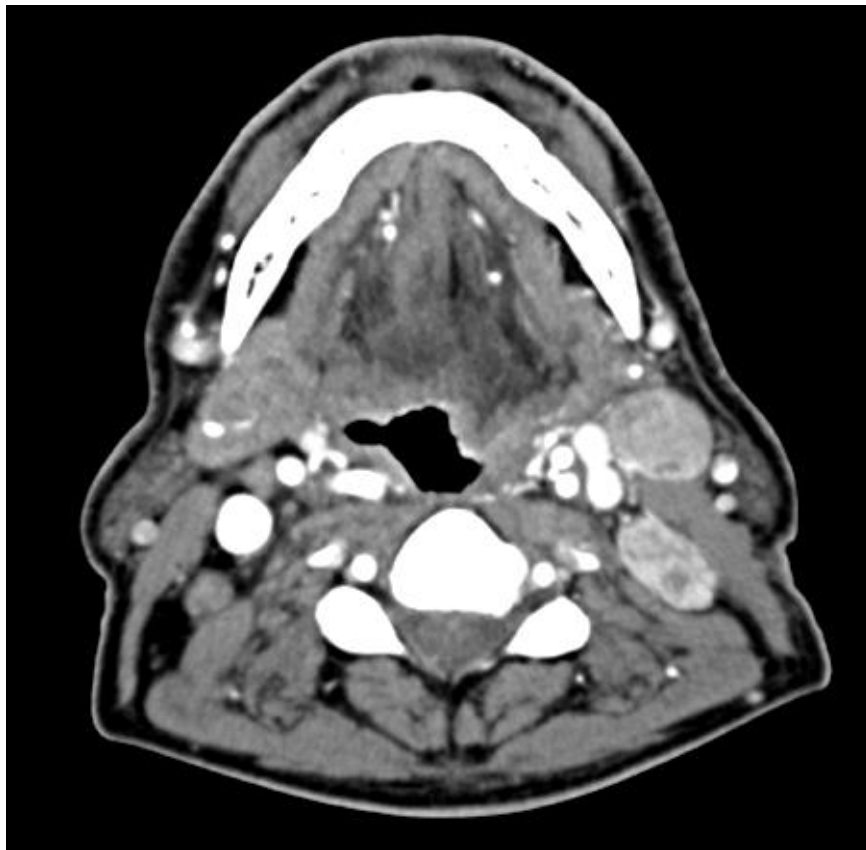
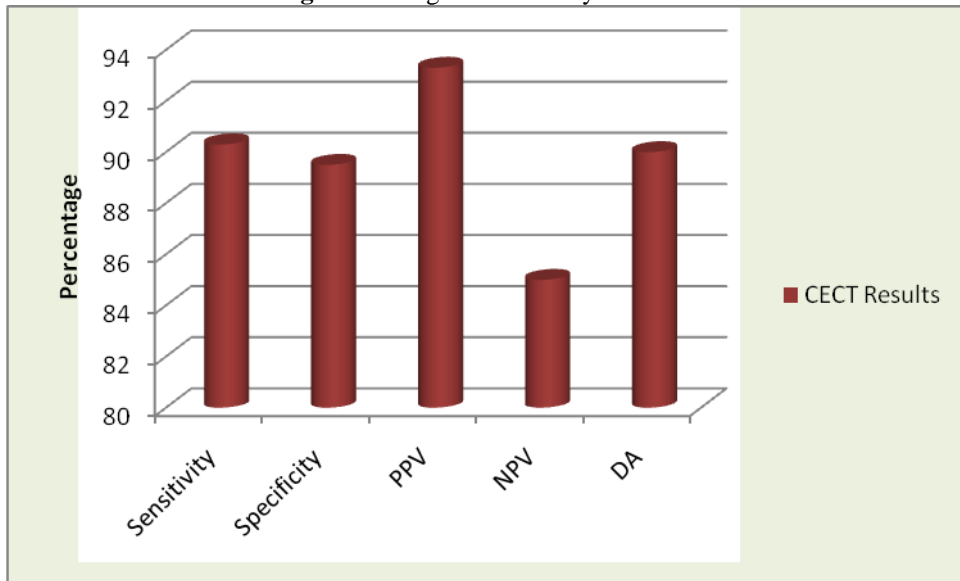


Image 1: 62 Yrs old male patient with FNAC proven Hodgkin's lymphoma. CECT axial image showing multiple necrotic ,homogeneous enhancing lymph nodes at level left IIA, IIB, right IIB



Image 2: 63 Yrs old male patient with FNAC proven benign non-TB (benign reactive hyperplasia).

CECT axial image showing large confluent, peripheral enhancing ,matted, necrotic, noncalcific level III bulging to III and IV lymph nodes on left side.

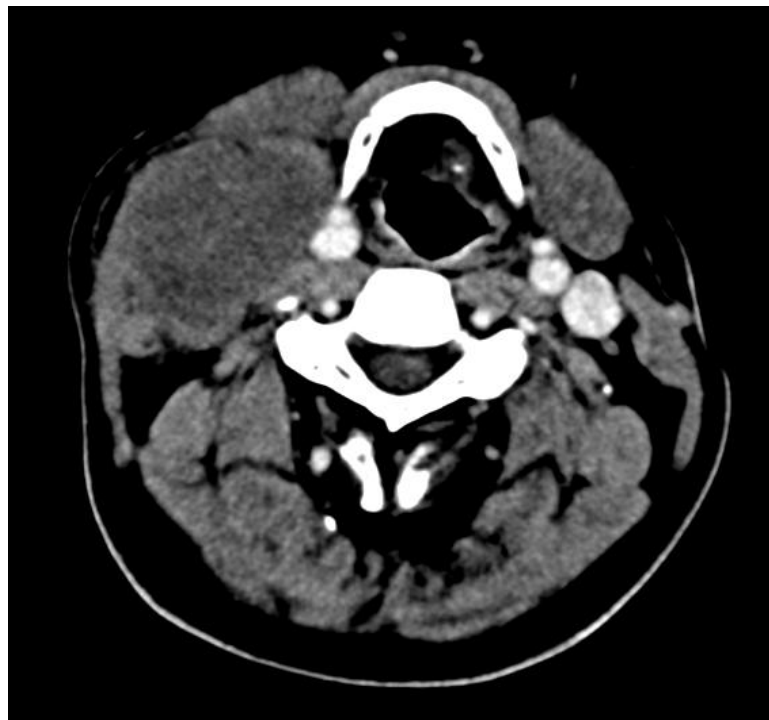
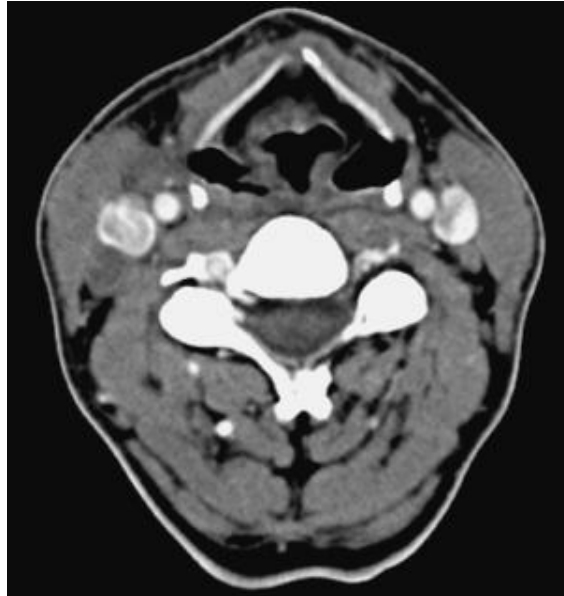
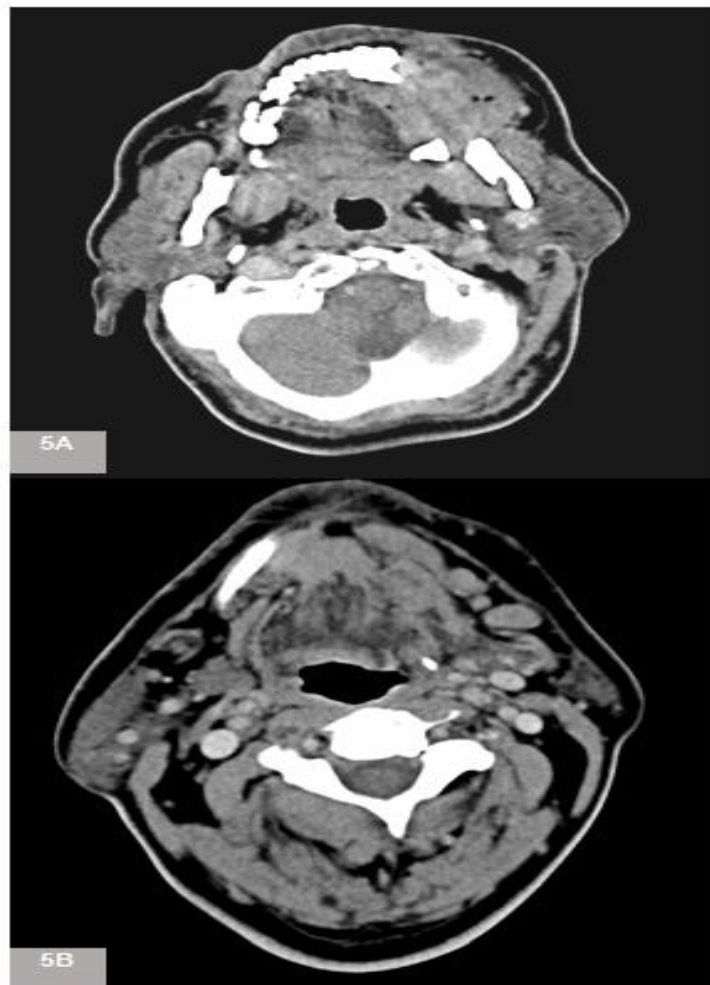


Image 3: 51 Yrs old male patient with biopsy proven metastatic CA.

CECT axial image showing peripheral enhancing, necrotic, matted right(RT) level IIA lymph node.



**Image 4: 75 Yrs old male patient with FNAC proven metastatic CA.
CECT axial image showing necrotic, noncalcific, well defined lymph nodes (arrow) on right side.**



**Image 5: Axial CT images of 56 Yrs old male patient with FNAC proven metastatic CA.
A-Image showing primary site of CA (large lobulated heterogeneously enhancing soft tissue mass involving left mandibular alveolus).
B- CT axial image showing multiple necrotic lymph nodes at level IB**